Theses and Dissertations   1. Thesis and Dissertation Collection, all items

1975

High frequency temperature fluctuations in the atmospheric boundary layer.

Simril, Robert Thomas

Monterey, California. Naval Postgraduate School

http://hdl.handle.net/10945/20886

HIGH FREQUENCY TEMPERATURE FLUCTUATIONS IN THE ATMOSPHERIC BOUNDARY LAYER

Robert Thomas Simril

NAVAL POSTGRADUATE SCHOOL
Monterey, California
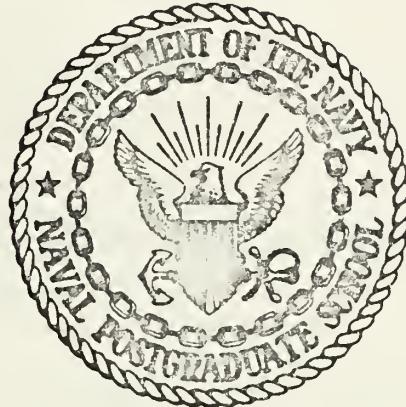
THESIS

HIGH FREQUENCY TEMPERATURE FLUCTUATIONS
IN THE ATMOSPHERIC BOUNDARY LAYER

by

Robert Thomas Simril

September 1975

Thesis Advisor: N. E. J. Boston

Approved for public release; distribution unlimited.

REPORT DOCUMENTATION PAGE		READ INSTRUCTIONS BEFORE COMPLETING FORM
1. REPORT NUMBER	2. GOVT ACCESSION NO.	3. RECIPIENT'S CATALOG NUMBER
4. TITLE (and Subtitle) High Frequency Temperature Fluctuations in the Atmospheric Boundary Layer		5. TYPE OF REPORT & PERIOD COVERED Master's Thesis; September 1975
		6. PERFORMING ORG. REPORT NUMBER
7. AUTHOR(s) Robert Thomas Simril		8. CONTRACT OR GRANT NUMBER(s)
9. PERFORMING ORGANIZATION NAME AND ADDRESS Naval Postgraduate School Monterey, California 93940		10. PROGRAM ELEMENT, PROJECT, TASK AREA & WORK UNIT NUMBERS
11. CONTROLLING OFFICE NAME AND ADDRESS Naval Postgraduate School Monterey, California 93940		12. REPORT DATE September 1975
		13. NUMBER OF PAGES 57
14. MONITORING AGENCY NAME & ADDRESS(If different from Controlling Office) Naval Postgraduate School Monterey, California 93940		15. SECURITY CLASS. (of this report) Unclassified
		15a. DECLASSIFICATION/DOWNGRADING SCHEDULE

16. DISTRIBUTION STATEMENT (of this Report)

Approved for public release; distribution unlimited.

17. DISTRIBUTION STATEMENT (of the abstract entered in Block 20, if different from Report)

18. SUPPLEMENTARY NOTES

19. KEY WORDS (Continue on reverse side if necessary and identify by block number)

Turbulence
Temperature Fluctuations
Atmospheric Boundary Layer
Kolmogorov Scalar Constant

20. ABSTRACT (Continue on reverse side if necessary and identify by block number)

Turbulent temperature fluctuations in the atmospheric boundary layer measured at 2m, 7m and 23m in Risø, Denmark, were analyzed with particular emphasis placed on determining characteristics of the high frequency region of the spectra of these fluctuations. The shape of the high wave number one-dimensional temperature spectrum and an estimate of the

Kolmogorov scalar constant were determined. Comparisons of high frequency spectral regions of temperature and velocity fluctuations were made.

High Frequency Temperature Fluctuations

in the Atmospheric Boundary Layer

by

Robert Thomas Simril
Lieutenant, United States Navy
B.S., North Carolina State University, 1969

Submitted in partial fulfillment of the
requirements for the degree of

MASTER OF SCIENCE IN OCEANOGRAPHY

from the

NAVAL POSTGRADUATE SCHOOL
September 1975

ABSTRACT

Turbulent temperature fluctuations in the atmospheric
boundary layer measured at 2m, 7m and 23m in Risø, Denmark,
were analyzed with particular emphasis placed on determining
characteristics of the high frequency region of the spectra
of these fluctuations. The shape of the high wave number
one-dimensional temperature spectrum and an estimate of the
Kolmogorov scalar constant were determined. Comparisons
of high frequency spectral regions of temperature and
velocity fluctuations were made.

.

TABLE OF CONTENTS

LIST OF FIGURES

LIST OF TABLES

ACKNOWLEDGEMENT

The author wishes to sincerely thank both Professors Noel E. J. Boston and Thomas M. Houlihan for their guidance and patience in overcoming the many obstacles encountered in the research involved in writing this thesis.

Special thanks go to my wife, Jan, for her patience, devotion and understanding.

Thanks to Tom, Dee and Deb, my children, for making it all worthwhile.

I. INTRODUCTION

Several attempts over the past few years have been made to measure high frequency temperature variations in the atmospheric boundary layer. Sensors with a sufficiently high frequency response and spatial resolution have been devised to overcome the inherent problems previously encountered in trying to measure small scale, high frequency temperature fluctuations. In addition to the sensitive sensors, low-noise electronic equipment has become available to record and analyze small scale fluctuations.

The object of this research was to utilize an analog analysis scheme to determine the shape of the high wave number (small scale) one-dimensional temperature spectrum and to evaluate the scalar constant, K_θ', which appears in the expression for the -5/3 form of the temperature spectrum. In addition, simultaneous analyses of velocity fluctuations were conducted in order to obtain the necessary information ultimately required to evaluate K_θ'.

A knowledge of the small scale temperature distribution in a turbulent field has a number of applications. It is necessary when considering the heat budget which is of utmost importance in the fields of oceanography and meteorology. Sensible heat flux can be determined by the covariance of measured temperature fluctuations and vertical components of the simultaneous wind velocity fluctuations.

10

Temperature inhomogeneities in the atmosphere are
one of the quantities associated with the scattering of
acoustic waves and electromagnetic radiation. This
scattering, which is a major concern in the fields of
acoustics and optics, is often related to variations in
the refractive index.

Further applications of a knowledge of the small scale
temperature distribution are found in the areas of physi-
cal chemistry and thermodynamics.

II. THEORETICAL DEVELOPMENT

A. VELOCITY SPECTRUM

Small scale turbulence in a fluid is a feature of interest to the environmental scientist due to its effect on heat, momentum and energy transport. The one-dimensional velocity (kinetic energy) spectrum is given by

$$\overline{u^2} = \int_0^\infty \Phi(k)dk \tag{1}$$

where $\overline{u^2}$ is the total variance of the turbulent velocity fluctuations and k is the radian wave number. The rate of energy dissipation in an isotropic, turbulent flow field is given by

$$\varepsilon = 15\nu \int_0^\infty k^2\Phi(k)dk \tag{2}$$

where the function $k^2\Phi(k)$, the dissipation spectrum, statistically describes the rate of decay of turbulent kinetic energy to heat. $\nu(cm^2.sec^{-1})$ is the kinematic viscosity of the fluid.

Modern turbulence research had as its impetus the concept of a continuous cascade of kinetic energy from large scale anistropic velocity fluctuations to smaller scales where the motion became increasingly isotropic and at which the energy is dissipated as heat. Small scale

12

motions which are characterized by small time scales are statistically independent of the relatively slow large scale turbulence derived from the mean flow.

This concept was presented by the Russian mathematician, A. N. Kolmogorov in 1941. Kolmogorov proposed the idea of local isotropy, i.e., at some point in the cascade of kinetic energy from large scales to small scales, the turbulent fluid motion becomes isotropic. This idea was described by Kolmogorov in two hypotheses:

(1) If the Reynolds Number (ratio of inertial to viscous forces) is sufficiently large, then there exists a range of small scales in which statistically, the turbulence is basically steady-state and is dependent only on the rate of dissipation of kinetic energy, $\varepsilon[(\text{cm/sec})^2 . \text{sec}^{-1})]$, the wave number, $k(\text{cm}^{-1})$ and the kinematic viscosity, $\nu(\text{cm}^2 . \text{sec}^{-1})$. Accordingly, dimensional analysis yields

$$\Phi(k) = (\varepsilon \nu^5)^{1/4} F(k/k_s) \tag{3}$$

for the form of the one-dimensional energy spectrum and

$$k^2 \Phi(k) = k_s^2 (\varepsilon \nu^5)^{1/4} (k/k_s)^2 F(k/k_s) \tag{4}$$

for the form of the energy dissipation spectrum. Here, $k_s = (\varepsilon/\nu^3)^{1/4}$ is the Kolmogorov wave number, $1/k_s$ is known as the Kolmogorov microscale. $F(k/k_s)$ is a universal function which is valid for all fields of turbulence provided the Reynolds Number is sufficiently large.

(2) If the Reynolds Number is very large (on the order of 10^6 and greater) then a range of scales exists wherein the energy cascades independent of viscosity. In this range of wave numbers, the decay of the flow energy is characterized by a -5/3 dependence upon wave number. This range in which the energy is transferred inertially is known as the inertial subrange and characterizes the turbulence scales too large to be influenced by viscosity but small enough to be separate from the mean flow. In the inertial subrange,

$$\Phi(k) = K'\varepsilon^{2/3} k^{-5/3} \tag{5}$$

where $\Phi(k)$ is the one-dimensional energy spectrum [$(cm/sec)^2 \cdot sec$] and K' is a universal constant. Previous researchers have reported values of K' ranging from 0.48 to 0.69 although the lower values are considered to be more accurate.

B. TEMPERATURE SPECTRUM

It is possible to apply the Kolmogorov ideas to turbulent fluctuations of passive scalars such as temperature. Temperature is a passive scalar when it is transported in a fluid but does not introduce buoyancy effects. If $\theta(C^\circ)$ is the deviation of the temperature from its

14

mean, the one dimensional temperature fluctuation spectrum
is defined as

$$\overline{\theta^2} = \int_0^\infty \Phi_\theta (k) dk \quad (C°)^2 . \tag{6}$$

The rate of temperature dissipation in an isotropic flow
field is

$$\varepsilon_\theta = 6\kappa \int_0^\infty k^2 \Phi_\theta (k) dk \quad (C°)^2 . sec^{-1} . \tag{7}$$

κ is the molecular diffusivity and $k^2 \Phi_\theta(k)$ is the scalar
dissipation spectrum which describes the distribution with
wave number of the rate of decay of the quantity θ^2, the
temperature variance.

Again, according to Kolmogorov:

(1) If the Reynolds number is sufficiently large there
exists a range of small scale temperature fluctuations which
statistically are dependent only on ε, ν, ε_θ (the tempera-
ture dissipation rate) and k. Once again dimensional
analysis yields

$$\Phi_\theta (k) = \varepsilon_\theta \varepsilon^{-3/4} \nu^{5/4} H(\sigma, k/k_s) \tag{8}$$

for the one-dimensional temperature spectrum and

$$k^2 \Phi_\theta (k) = k_s^2 \varepsilon_\theta \varepsilon^{-3/4} \nu^{5/4} (k/k_s)^2 H(\sigma, k/k_s) \tag{9}$$

15

for the temperature dissipation spectrum. σ is the Prandtl number ($\sigma = \nu/\kappa$), the ratio of kinematic viscosity to thermal diffusivity. In a gas σ is approximately 1. For air at 20°C the value is near 0.7.

(2) If the Reynolds Number is even larger, then the temperature spectrum is independent of ν and κ and is determined only by ε and ε_θ. Dimensional analysis [Corrsin, 1951] yields

$$\Phi_\theta(k) = K_\theta' \varepsilon_\theta \varepsilon^{-1/3} k^{-5/3}. \tag{10}$$

K_θ' is supposedly a universal constant although previous researchers have reported values ranging from 0.2 to 2.0.

In view of this range of reported values of K_θ' it was the intent of this research to determine the shape of one-dimensional temperature spectra at high wave numbers and to evaluate K_θ' from the data analyzed. In this way, a larger data base could be established from which determinations for K_θ' could be resolved.

III. INSTRUMENTATION AND EXPERIMENTAL APPROACH

A. BACKGROUND

Sensors and electronic systems with the necessary sensitivity and response to measure high frequency, small scale atmospheric temperature fluctuations were developed in the early 1970's by National Electrolab Associates Limited of Vancouver, British Columbia, in consultation with the Institute of Oceanography, University of British Columbia. Previous electronics allowed the temperature spectrum to be measured to just beyond the inertial sub-range but not to sufficiently high wave numbers to unequivocally evaluate the area under the scalar dissipation spectrum.

B. TEMPERATURE MEASURING SYSTEM

1. Sensor

The sensor of temperature fluctuations utilized was a resistance thermometer consisting of a platinum wire 0.25 μm (0.00001 in.) in diameter and 0.30 mm in length. The wire has a time constant of less than 10 μs in a 4 m/sec air flow. With a detection current of 50 μamps, its sensitivity is 0.063 mv/°C. The sensor is made from Wollaston wire consisting of a silver jacket about a platinum core. The outside diameter of the jacket is 45 μm (0.0018 in.). The jacket and core are prestressed

into a V-shape and then soldered onto the end of a standard hot wire anemometer probe (Figure 1). The sensor has a frequency response which is essentially flat to 5KHz.

2. Bridge

Utilizing a thin platinum wire to measure temperature fluctuations takes advantage of the fact that a slightly heated wire is basically a simple resistance thermometer. In order to sense a change in resistance in the wire due to variations in the ambient temperature, a small heating current is passed through the wire and the resulting voltage drop can be measured. If the heating is kept low, the resistance changes due to cooling by wind are negligible compared to resistance changes caused by temperature fluctuations. A bridge circuit is utilized to ensure optimum current flow through the platinum core.

The bridge circuit is a modified Wheatstone bridge consisting of two 2.21KΩ resistors, sensor, probe and cable, balance adjustment resistors and capacitors. The fixed and variable capacitors (Figure 2) paralleling the balance resistance are necessary to match the probe and cable capacitance. The bridge amplifier is a differential amplifier with a fixed gain of 60dB and a frequency response flat to 150KHz.
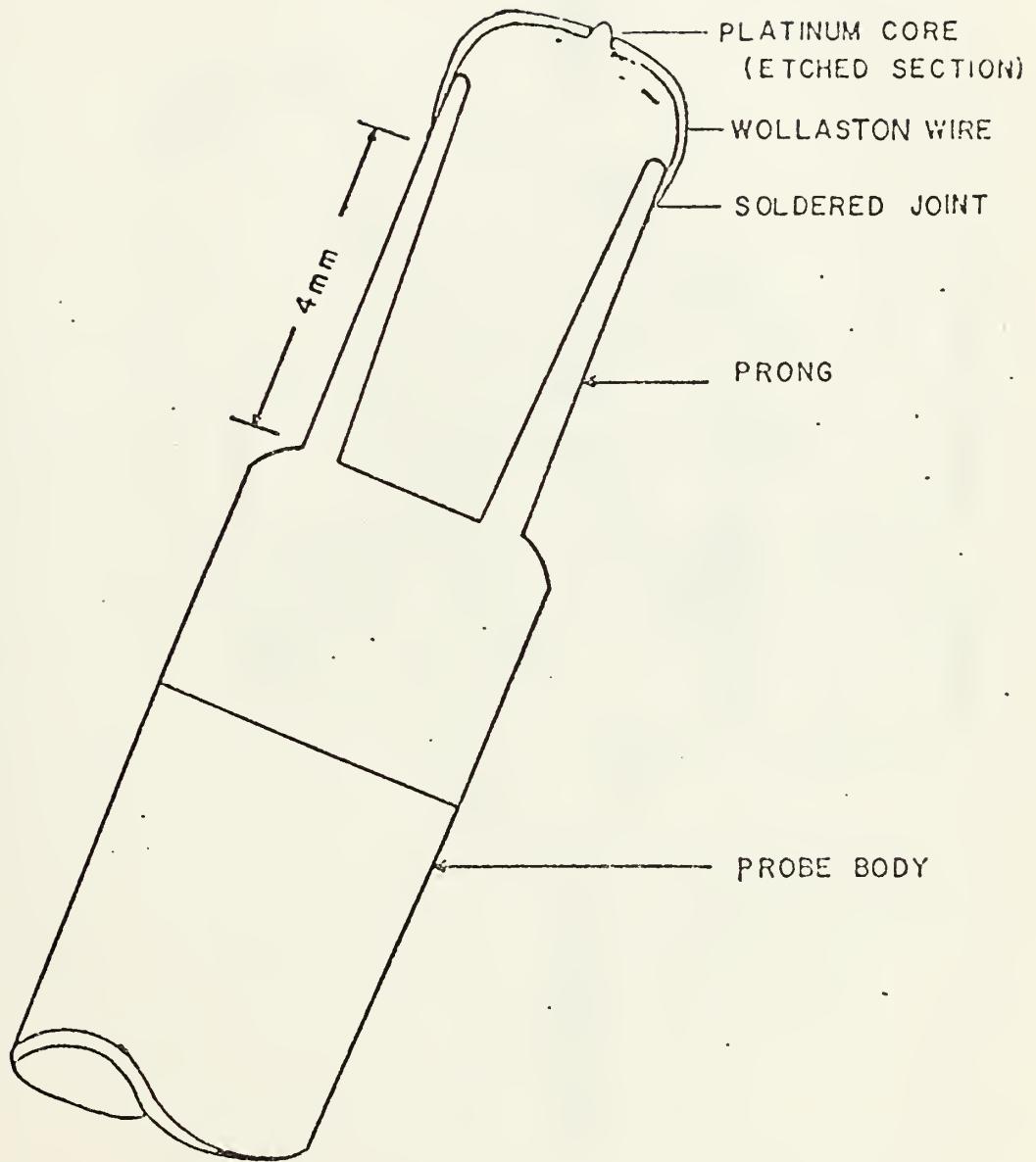
Figure 1.   Wollaston Wire Mounted on Probe
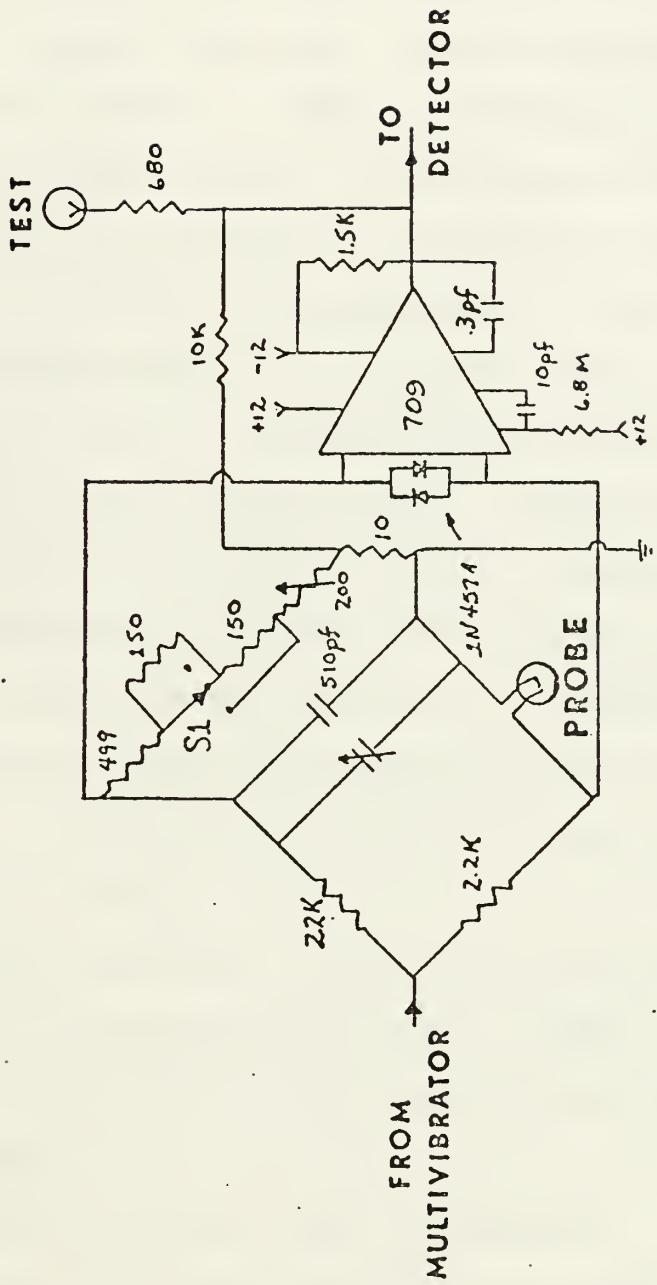
Figure 2. Bridge Circuit

20

C. EXPERIMENTAL PROCEDURE

1. Location

The data were collected at the meteorological field site operated by the Meteorological Group of the Danish Atomic Energy Commission, Research Establishment, Risø. The site features a 130M meteorological tower instrumented at seven levels. In addition, miscellaneous instrumentation can be mounted at arbitrary levels provided only that the electronics is sufficient to drive the cables from the instrumentation to the junction boxes at the seven standard levels. The tower stands on the Risø Peninsula 0.5 Km from Roskilde Fjord. Signals from tower instrumentation are carried by cable to a meteorological station 50m downwind of the tower where both analog and digital recording equipment are housed. During the course of the experiments winds blew essentially from the west off the fjord. Data were not collected unless the wind was from off the water.

The Risø Peninsula is 6Km north of the ancient Danish town of Roskilde which in turn is 30Km approximately southeast of Copenhagen on the island of Sjaelland.

2. Equipment

a. Meteorological Tower Arrangement

Mean wind speed and direction, temperature and humidity were measured at 7, 23, 39, 56, 72 and 96m (Figure 3). Sonic anemometer measurements were made at

21
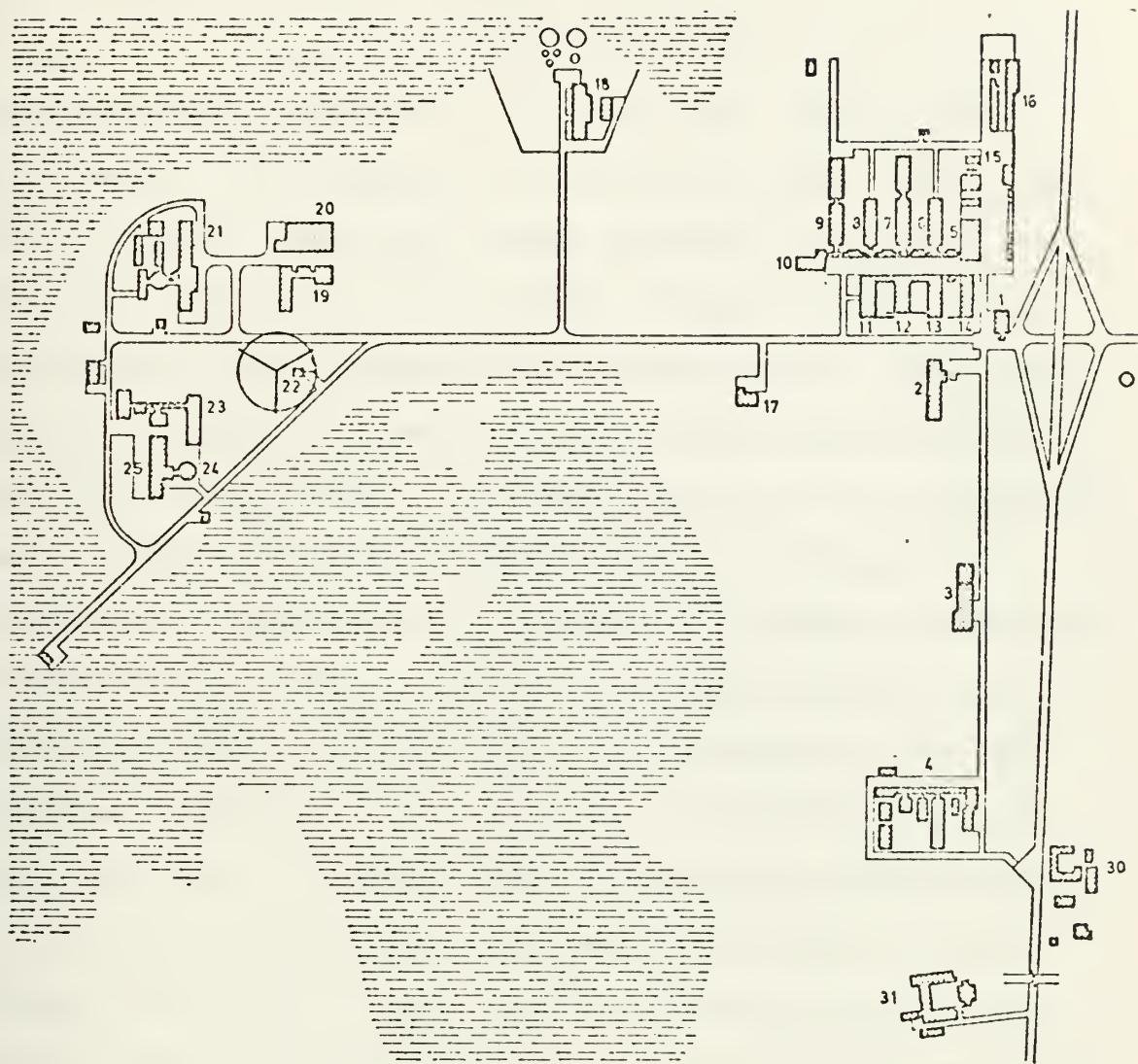
1. Gate-house and fire
   station
2. Administration
3. Accelerator Department
4. Agricultural Department
5. Workshop
6. Physics Department
7. Electronics Department
8. Reactor Physics
   Department
9. Chemistry Department
10. Lecture Hall
11. Canteen

12. Library
13. Health Physics
    Department
14. Engineering Department
    and drawing offices
15. Helium plant
16. Service and maintenance
17. Research Reactor DR 1
18. Waste treatment plant
19. Metallurgy Department
20. Hot Cells
21. Research Reactor DR 3
22. Meteorology station

23. Isotope Laboratory
24. Research Reactor DR 2
25. Reactor Engineering
    Department
26. Tandem Accelerator
    Department of the
    Niels Bohr Institute
27. Kindergarten
28. Guest-house
29. Staff dwellings
30. "Svaleholm" farmhouse
31. "Dyskærgård" farmhouse

Figure 3.   Risø Research Establishment

2, 23 and 72m. Fine structure turbulence measurements
were made at different heights during the course of the
experiment. In general, Naval Postgraduate School (NPS)
equipment was deployed at 2m, 7m or 23m. Oregon State
University (OSU) equipment was always at 23m. University
of California, San Diego (UCSD) equipment was placed very
near the top of the mast at 123m. Danish Atomic Energy
Commission (AEK) equipment was located at 2m. Each group
deployed sensors for measuring turbulent temperature and
velocity fluctuations. The main purpose of the experiment
was to make simultaneous measurements of atmospheric
temperature fluctuations by different systems, at the same
level and at different levels. The temperature sensor in
each case was a platinum wire. The diameter of the NPS
wire was 0.25 μm, of OSU 0.625 μm and of UCSD both 0.25
and 0.625 μm. By making these simultaneous measurements
with similar sensors but different electronics, it was
hoped (1) to find in what way they differed and (2) more
importantly, to resolve some of the discrepancies surround-
ing the value of the scalar constant K_θ'.

The main comparisons made in this thesis are
between the NPS and OSU systems.

b. NPS Platinum Resistance Thermometer

At the 2m height the sensor was mounted in an
aluminum holder which could hold as many as four such
sensors. For the data discussed in this thesis the

temperature sensor was placed 5mm below a Disa hot wire
anemometer. The other two positions were left vacant.

At 7m the same aluminum holder was used but a
Thermosystems probe was used for the hot wire. This probe
was vertically aligned and then rotated to be within 5mm
to the side of the temperature sensor.

A somewhat similar arrangement was made at
23m except it was more difficult to get the temperature
probe close to the hot wire probe. There was a separation
of approximately 1cm.

c. Hot Wire Anemometer

A variety of hot wire anemometers was used.
They were Disa (AEK, UCSD), Thermosystems (NPS, OSU),
and a new wind-vane probe system (AEK) designed by Larsen
and Busch (1974).

Disa probes were mounted in the aluminum holder
previously described whereas the other systems had indi-
vidual clamps.

3. Recording Systems

NPS, OSU and UCSD used analog tape recorders.
AEK recorded digitally on magnetic tape. The NPS data
analyzed for this thesis were recorded on an Ampex FR 1300
tape recorder at 7 1/2 ips using FM electronics. At this
speed the 3dB point is at 2.5KHz. Each NPS temperature
signal was recorded both direct and differentiated (with
respect to time). The object of the differentiation is

to increase the level of the signal at high frequencies above the noise level. The differentiator circuit had a gain of 6dB/octave over the differentiating band of frequencies. This band could be varied from DC to 500Hz, 1000Hz, 1500Hz, 2000Hz or 3000Hz. The frequency at which unity gain occurred could also be varied. Beyond the band of differentiation, the circuit rolled off at 6dB/octave. No other filtering of the signals was done. NPS hot wire signals were recorded directly without filtering or differentiation.

The input level of the tape recorder was set to handle 1 volt rms signals.

IV. ANALYSIS PROCEDURES

A. SELECTION OF DATA

Generally when concerned with the analysis of high frequency turbulent temperature and velocity signals, it is not necessary to examine long sections of data. It was determined, however, in the preliminary analysis of this data that in order to obtain characteristic spectra, it would be necessary to extend the record length to 10 minutes. This was due to varying levels of the recorded signals, necessitating the utilization of a broadband amplifier to maintain the signal level at an almost constant level.

The primary considerations for selecting a section of data for analysis were first that the temperature and velocity fluctuations be considered typical of the record and secondly, if possible, correspond to sections that were being analyzed at Oregon State University for future comparison of results (Figure 4). By trying to adhere to these considerations, the following data sections were analyzed: a 10 minute length of record from Run 5 commencing at 1537 local Risø time on 30 August 1974, and a 10 minute length of record from Run 6 commencing at 1657 on 30 August 1974 (Table I).
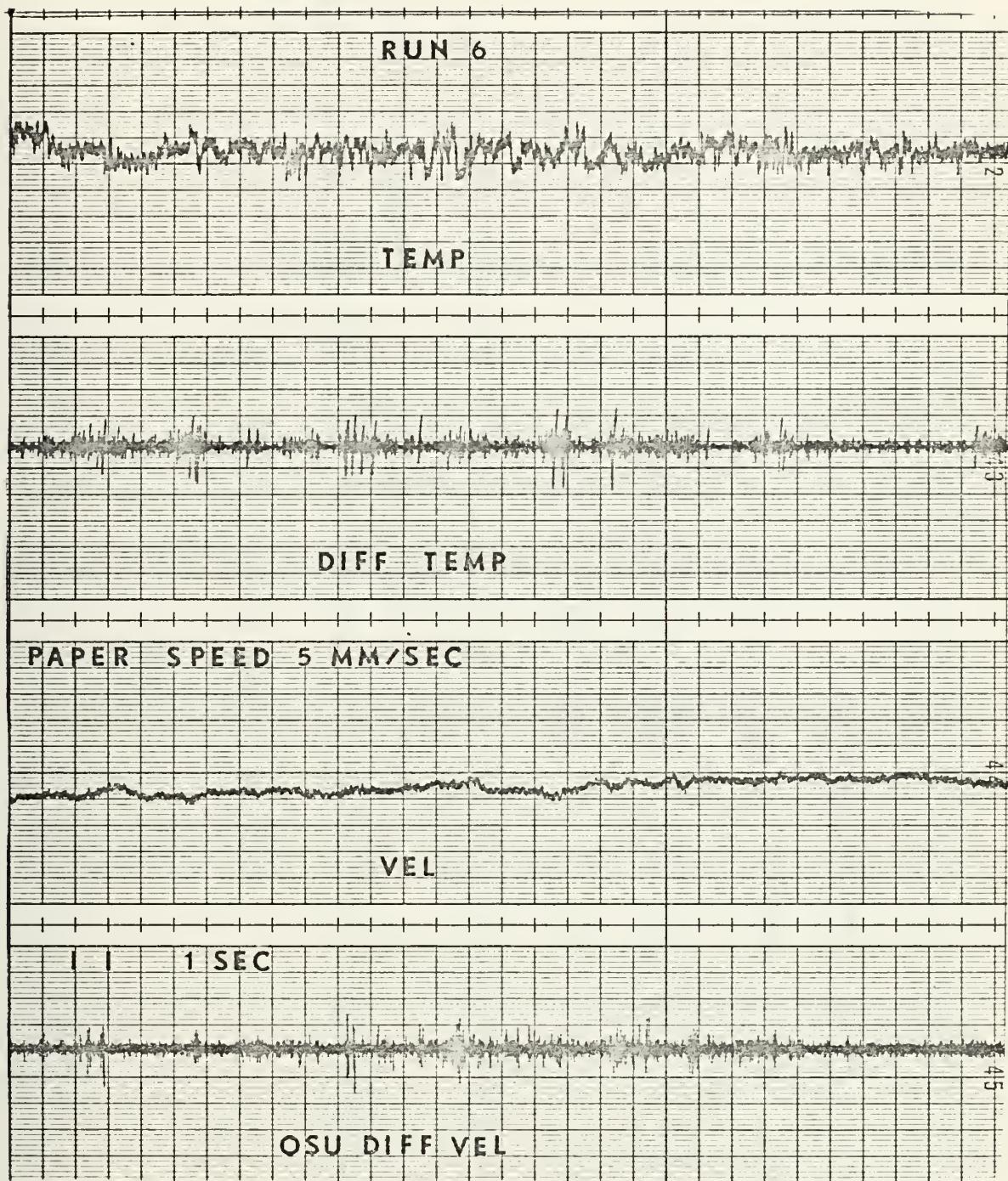
Figure 4. Example of Data Selected for Analysis

27

TABLE I

LISTING OF SECTIONS ANALYZED

Tape No.	Run	Mean Wind Speed (cm/sec)			Length of Record
		2m	7m	23m	
2	5	394	448	500	10 min.
2	6	386	428	467	10 min.

Note 1: Run 5 commenced at 1537.

Note 2: Run 6 commenced at 1657.

B. ANALOG EQUIPMENT AND PROCEDURES

The analog analysis scheme consisted of utilizing the following state-of-the-art equipment to obtain spectra of the selected sections (Figure 5):

A Honeywell Model Ninety-Six Magnetic Tape Recorder/ Reproducer System was used to playback the recorded signals. This device is capable of recording/reproducing any combination of multi-channel direct (analog) and FM data at nine selectable servo-controlled tape speeds from 15/16 through 240 inches per second (ips). Its standard magnetic assemblies are IRIG compatible. It is characterized by a tape speed accuracy of 0.1% and a bandwidth of 0-2.5KHz (within 1dB) at a signal-to-noise ratio of 50dB when operated at 7-1/2 ips.

The playback signals from the reproducing system were fed to a Preston 8300 XWB Amplifier with a bandwidth of 100KHz and selectable gains of 1, 2, 5, 10, 20 and 50.

The output from the amplifier was fed into the input of a Federal Scientific UA-500 Ubiquitous Spectrum Analyzer. The selected analysis range was 0-2KHz at a sample rate of 6000hz. The analyzer has a 3dB bandwidth of 6hz and a frequency accuracy of ±0.2% of the full analysis range.

The input signal to the analyzer was monitored by a Hewlett-Packard 3400A RMS Responding Voltmeter and a Tecktronix Type 502A Dual-Beam Oscilloscope.
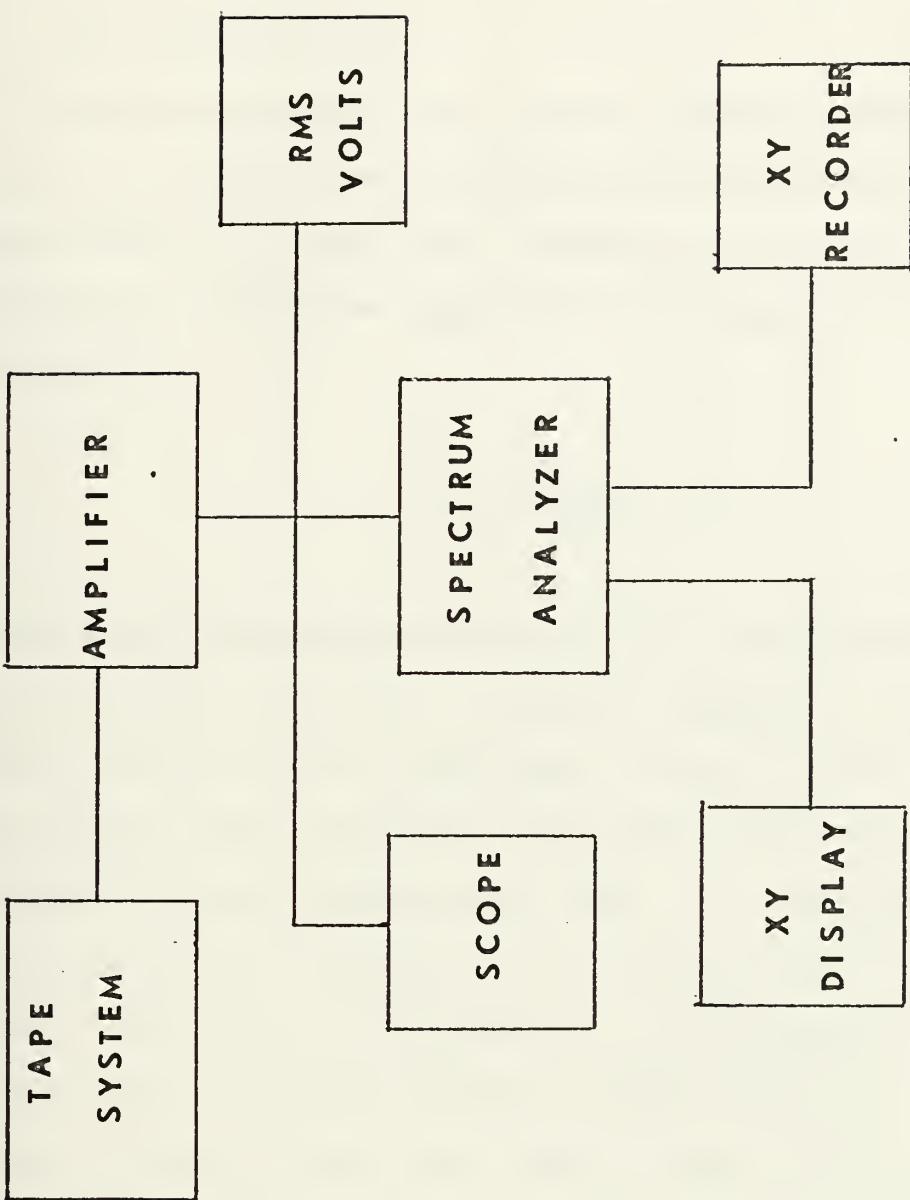
Figure 5. Analog Analysis Scheme

The spectral output was visually monitored on a
HP 1300A X-Y Display and plotted on a Mosely 7035B X-Y
Solid State Recorder produced by Hewlett-Packard.

C. DATA INTERPRETATION

Theoretical work almost always expresses turbulence
results in terms of wave number while actual turbulence
measurements are spectrally computed as functions of
frequency. These two approaches are related by Taylor's
hypothesis

$$k = \frac{2\pi f}{U} \tag{11}$$

where k is radian wave number (cm^{-1}), f is frequency (Hz)
and U is mean wind speed (cm/sec). Equation 11 implies
that turbulence with scales near 1/k are "frozen" during
the period these scales are swept past the sensor. The
maximum frequency analyzed was 2KHz at a mean wind speed
of 5 m/sec which indicated that a maximum wave number of
$25cm^{-1}$ would have to be resolved. This requires that the
sensor does not exceed 0.4mm in length and have a fre-
quency response essentially flat to 2KHz. Both of these
requirements were met.

Since Eq. 11 is linear, the shape of a wave number
spectrum is the same as that of a frequency spectrum.
Frequency spectra and wave number spectra are related by

$$f\phi(f) = k\phi(k) \ . \tag{12}$$

The inertial subrange expression (eq. 5) in terms of f becomes

$$\phi(f) = (\frac{2\pi}{U})^{-2/3} K'\epsilon^{2/3} f^{-5/3} \ . \tag{13}$$

The rate of kinetic energy dissipation expression (eq. 2) becomes

$$\epsilon = 15\nu \ (\frac{2\pi}{U})^{2} \int_{0}^{\infty} f^{2}\phi(f)df \ . \tag{14}$$

The resulting expressions for the temperature spectrum in terms of f are

$$\phi_\theta(f) = (\frac{2\pi}{U})^{-2/3} K_\theta'\epsilon_\theta \epsilon^{-1/3} f^{-5/3} \tag{15}$$

and

$$\epsilon_\theta = 6\kappa \ (\frac{2\pi}{U})^{2} \int_{0}^{\infty} f^{2}\phi_\theta(f)df \ . \tag{16}$$

Equations 13, 14, 15 and 16 were the expressions used to evaluate ϵ, ϵ_θ and K_θ'.

V.   RESULTS

A.   VELOCITY SPECTRUM RESULTS

1.   Calculation of ε

a.   Indirect Method

An indirect estimate of ε was made from the friction velocity and the logarithmic wind profile (Figure 6).   Thus,

$$U_* = KU/\ell N \; \frac{Z + Z_0}{Z_0} \tag{17}$$

where $K = 0.4$ is the von Karman constant and Z_0 the roughness length.   The relation

$$\varepsilon = U_*{}^3/KZ \tag{18}$$

was then used to evaluate ε.

b.   Inertial Range Method

Once the spectrum $\phi(f)$ was determined, ε was estimated by choosing values of $\phi(f)$ from the best straight line in the frequency region in which a $-5/3$ form was observed and then substituting into Eq. 13.   A value of 0.5 was assumed for the constant K' based on results presented by Boston (1970) and Williams (1974).

c.   Direct Method

The kinetic energy dissipation rate was estimated directly by summing of the frequency range

33
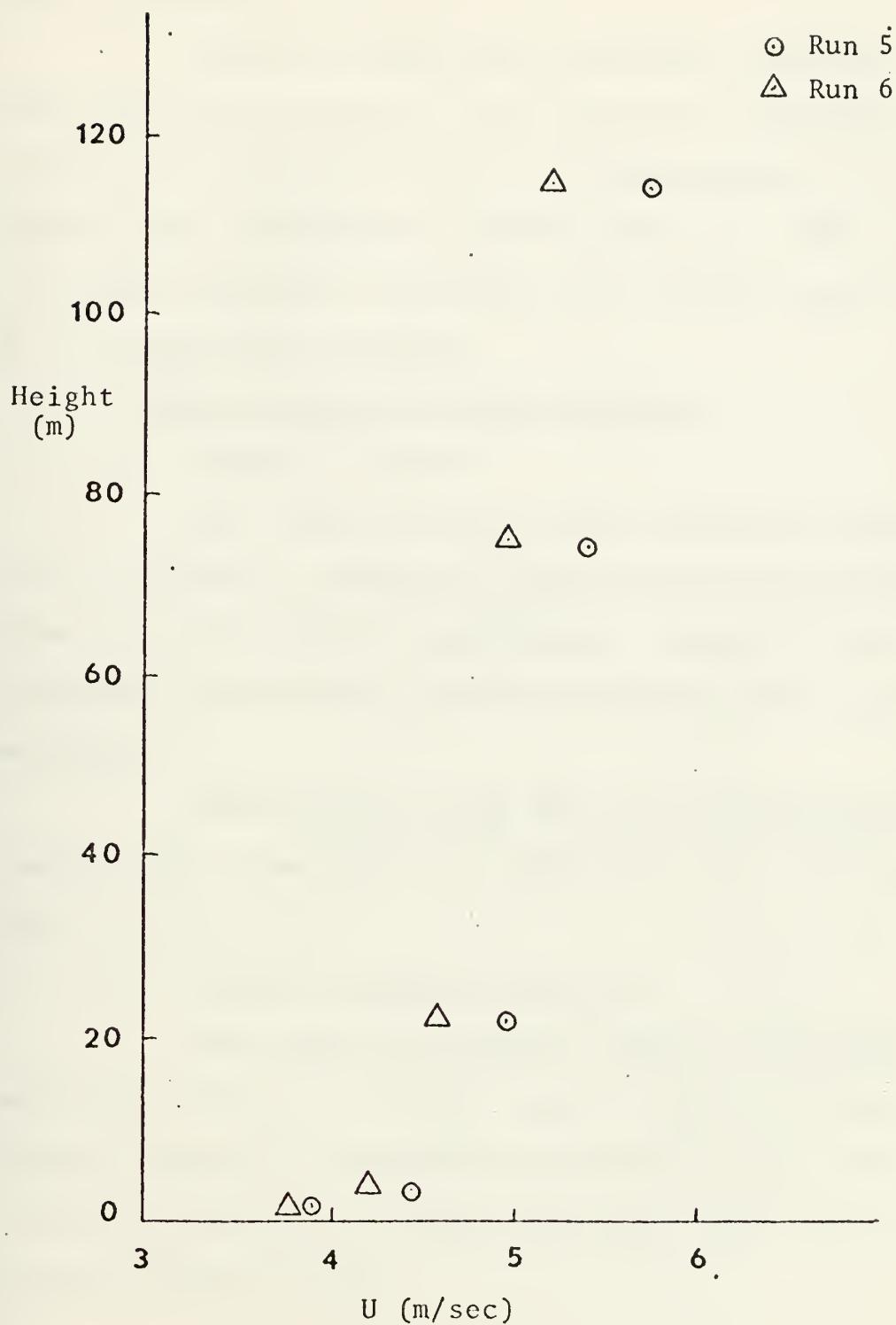
Figure 6. Wind Profiles Runs 5 and 6

from 10Hz to 2KHz the scales contributing to viscous dissipation according to Eq. 14.

Table II summarizes the results obtained from these three methods. All values of ε determined by the three methods were felt to be representative of the actual value. Therefore an average value for each run at a given height was utilized in the further analysis of the temperature spectrum.

2. Normalization of Spectral Results

a. Velocity Spectra

The velocity spectra were normalized according to Eq. 3 so that a comparison could be made between different runs and previous experiments. Figures 7 and 8 are normalized velocity spectra from Runs 5 and 6 at the 2m height.

These figures show that the spectra nearly overlap with a characteristic break from the -5/3 region near $\log k/k_s = -1$.

b. Energy Dissipation Spectra

The energy dissipation spectra were normalized according to Eq. 4. A linear plot was used to display results (Figure 9). Maximum dissipation occurred near the value of $k/k_s = 0.1$ which is in agreement with previous research [Boston, 1970].

TABLE II

COMPARISON OF ε VALUES

	U(cm/sec)	ε (ID)	ε (IR)	ε (D)
Run 5				
2m	394	3132	3069	3029
7m	448	484	447	473
23m	500	86	105	96
Run 6				
2m	386	2445	2526	2381
7m	428	312	311	287
23m	467	56	58	61

Figure 7.   Normalized NPS Velocity Spectrum Run 5 at 2m
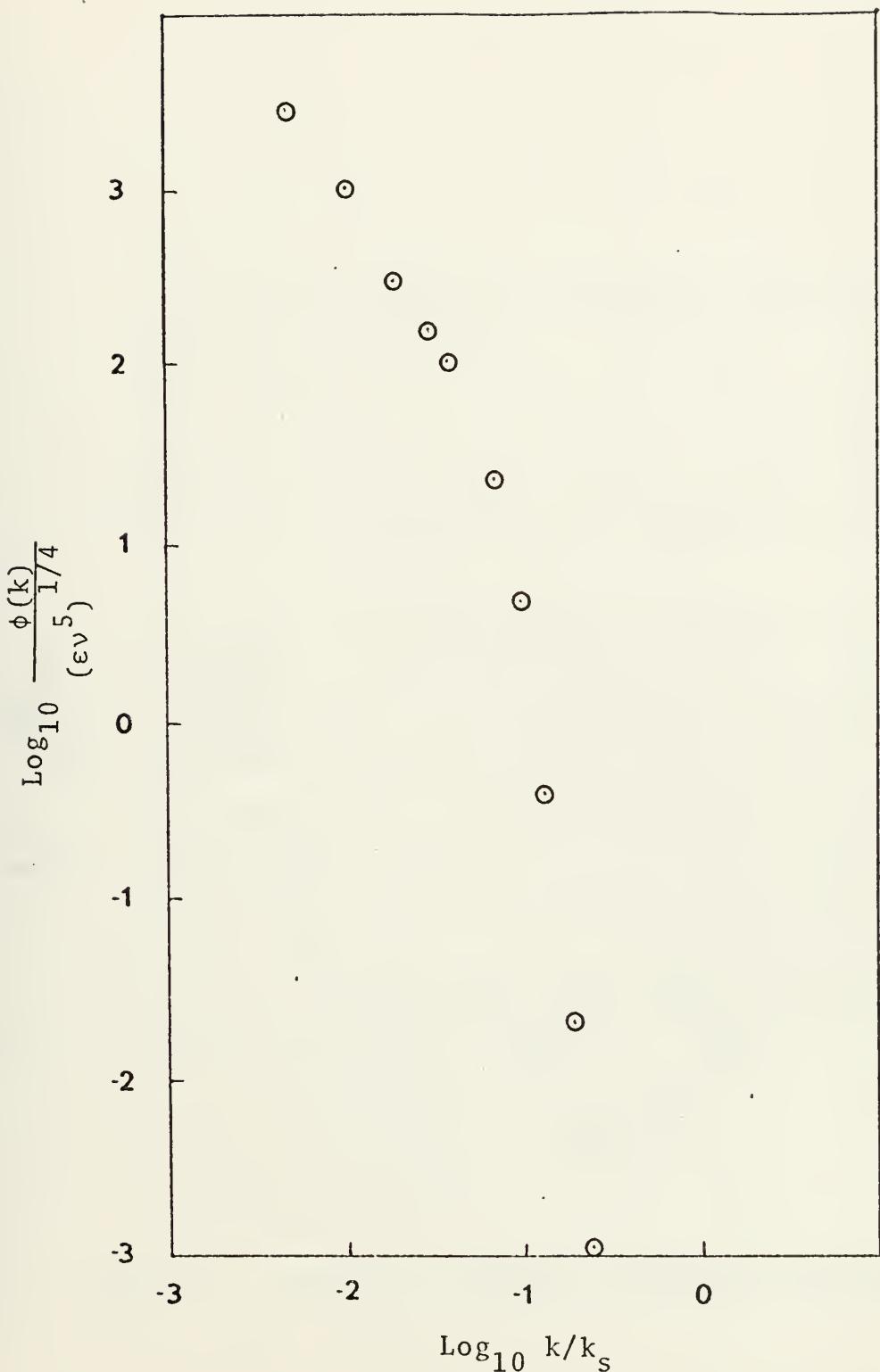
Figure 8. Normalized NPS Velocity Spectrum Run 6 at 2m

38
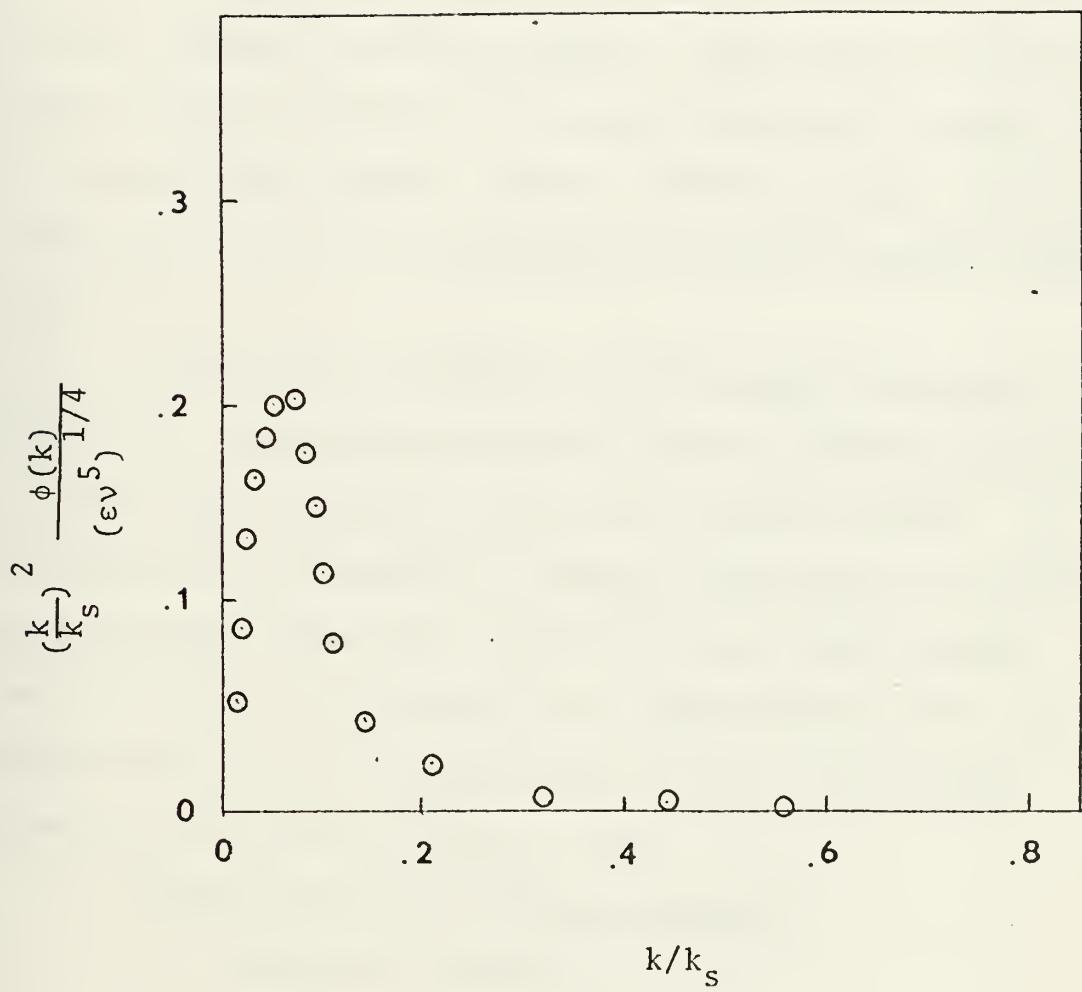
Figure 9. Normalized Energy Dissipation Spectrum

B. TEMPERATURE SPECTRUM RESULTS

1. Calculations of ε_θ

ε_θ values were estimated from Eq. 16 and the results are included in Table III.

2. Calculations of K_θ'

The values of K_θ' were determined from Eq. 15. Values of $\Phi_\theta(f)$ were chosen from the best straight line in the frequency region in which a -5/3 form was observed. The value of ε used was the average value for a given run at a particular height. Since ε enters into Eq. 15 to the -1/3 power, errors in estimating ε do not seriously affect K_θ'.

The results of the K_θ' calculations are shown in Table III. An average value of 0.88 was obtained which is in quite good agreement with 0.81 by Boston (1970). It was noted that although no inherent differences in temperature spectral shape were observed between OSU and NPS sensor results, the values of K_θ' determined at the 23m height from the OSU sensors were very near the values reported by Williams (1974) at OSU.

3. Normalization of Spectral Results

a. Temperature Spectra

The temperature spectra were normalized according to Eq. 8. The temperature spectra from each run at each height were normalized and plotted (Figures 10-15). A composite spectrum was obtained by superimposing
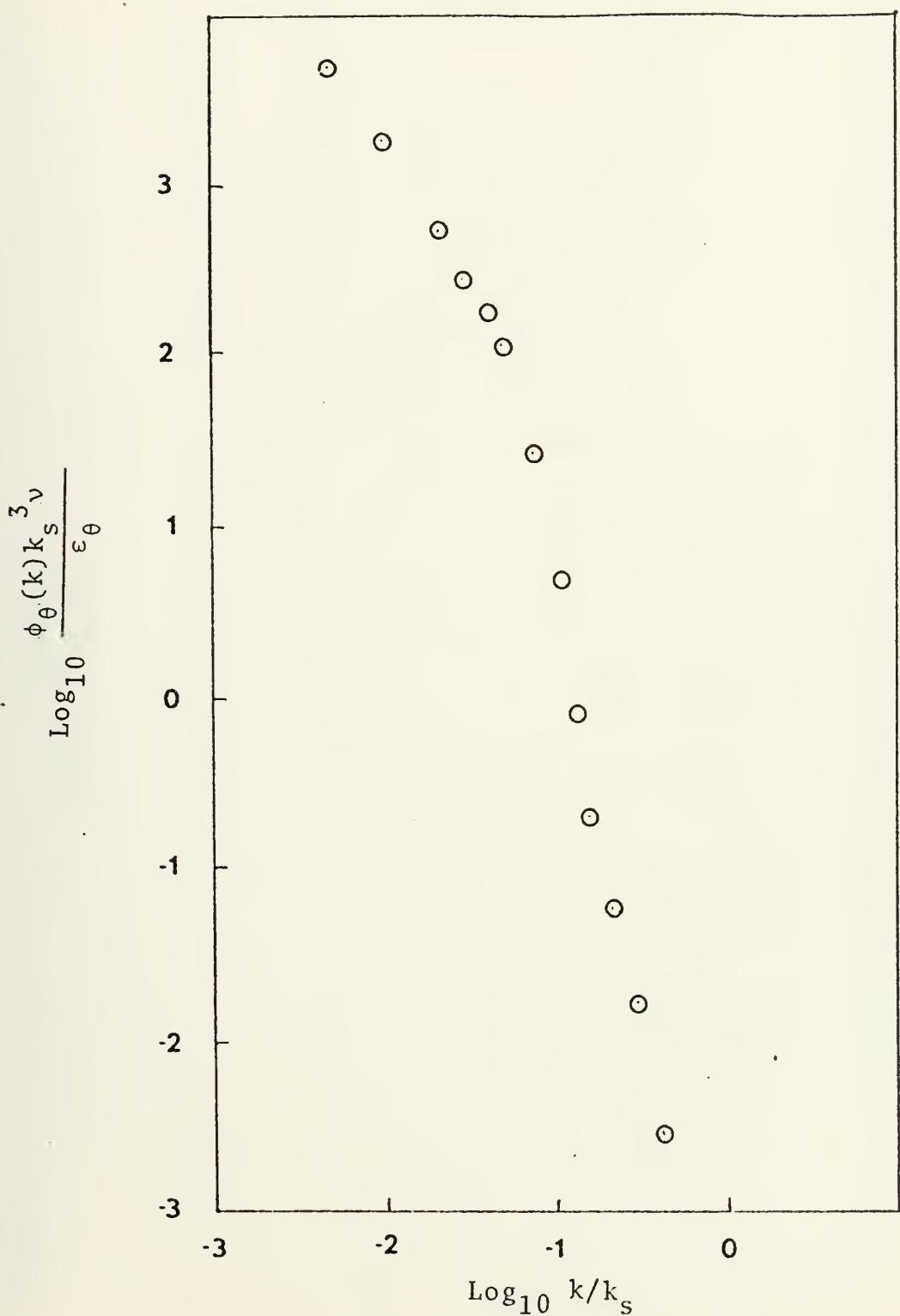
Figure 10.   Normalized NPS Temperature Spectrum Run 5 at 2m

41
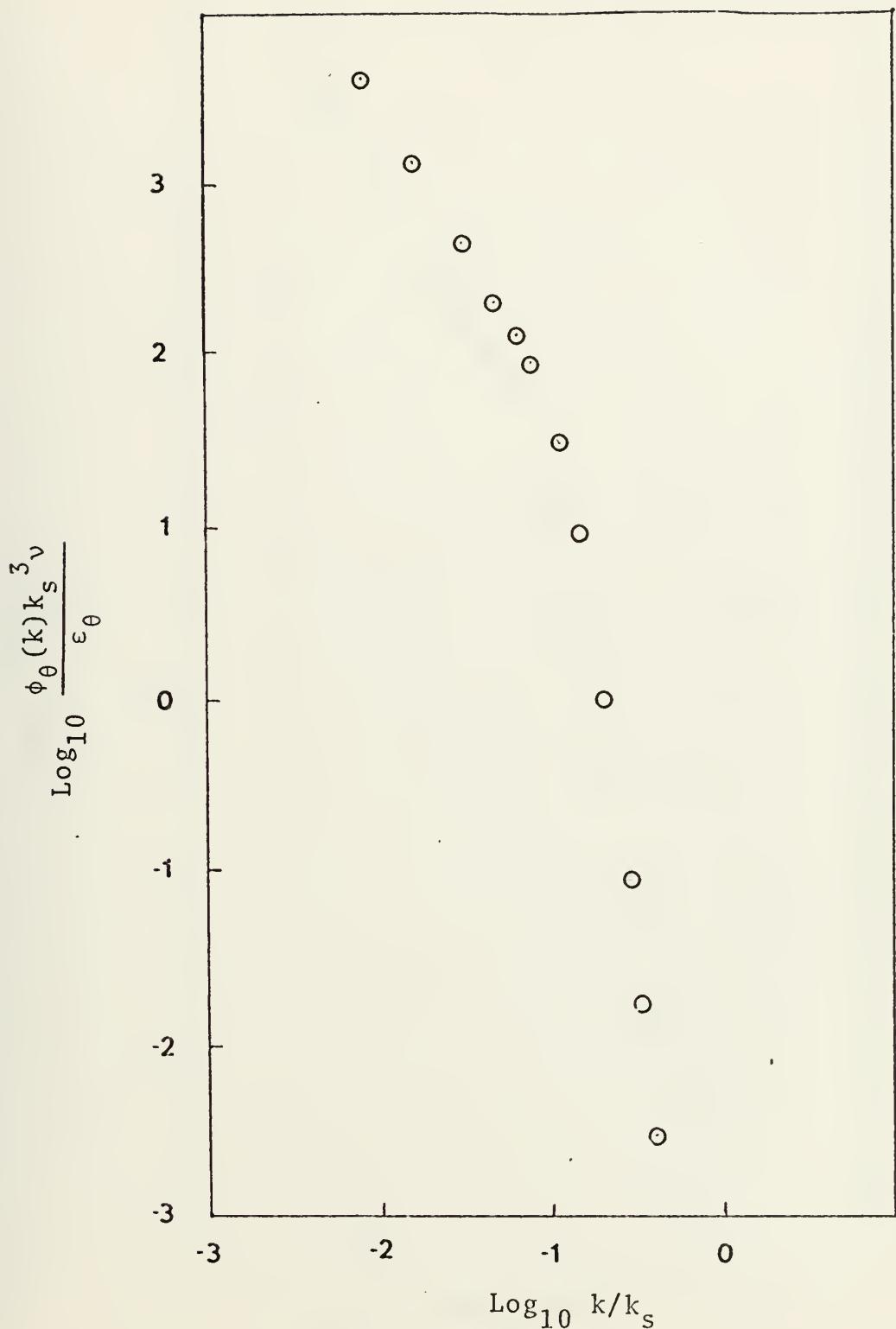
Figure 11.   Normalized NPS Temperature Spectrum Run 6 at 2m
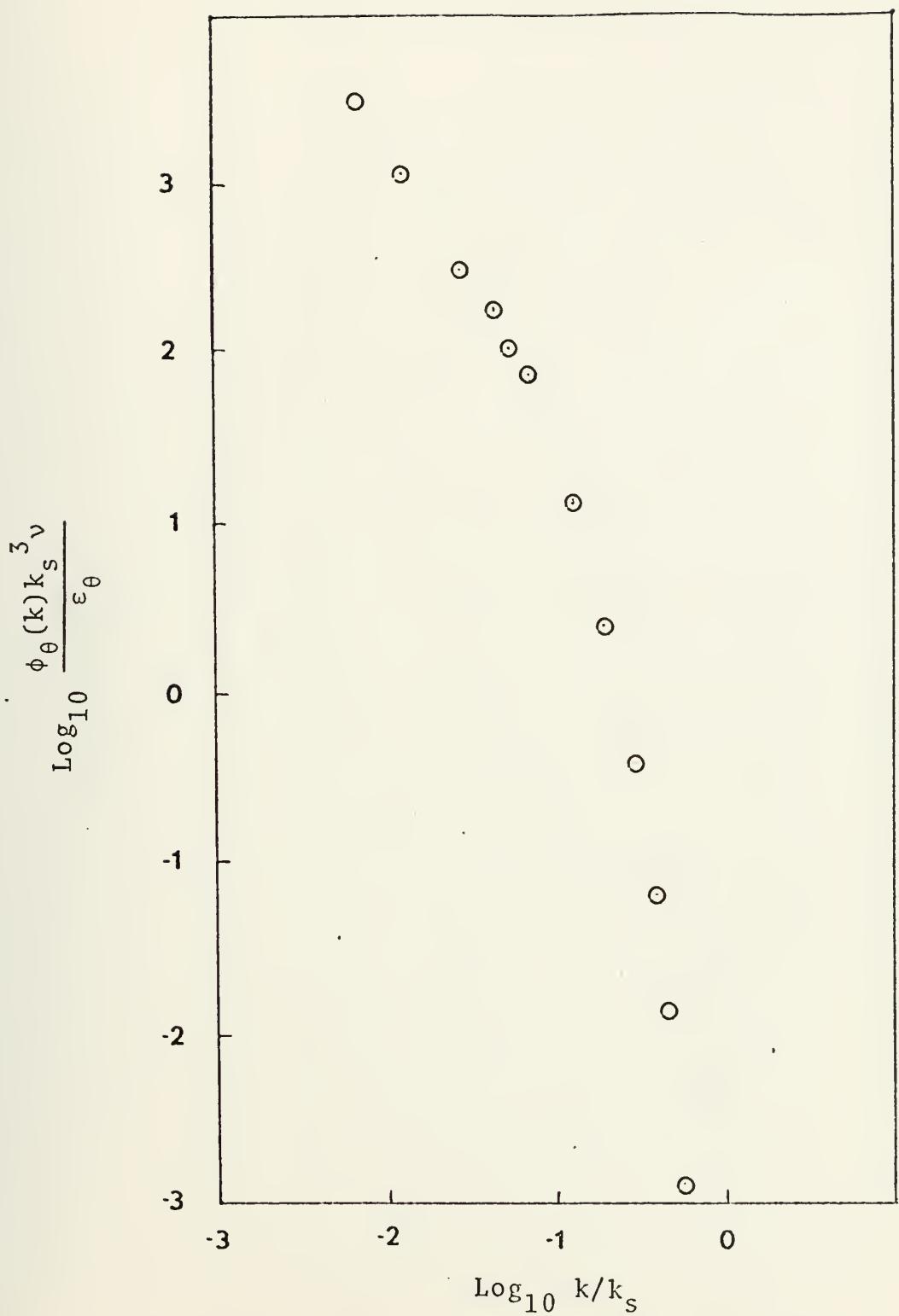
Figure 12. Normalized NPS Temperature Spectrum Run 5 at 7m

43
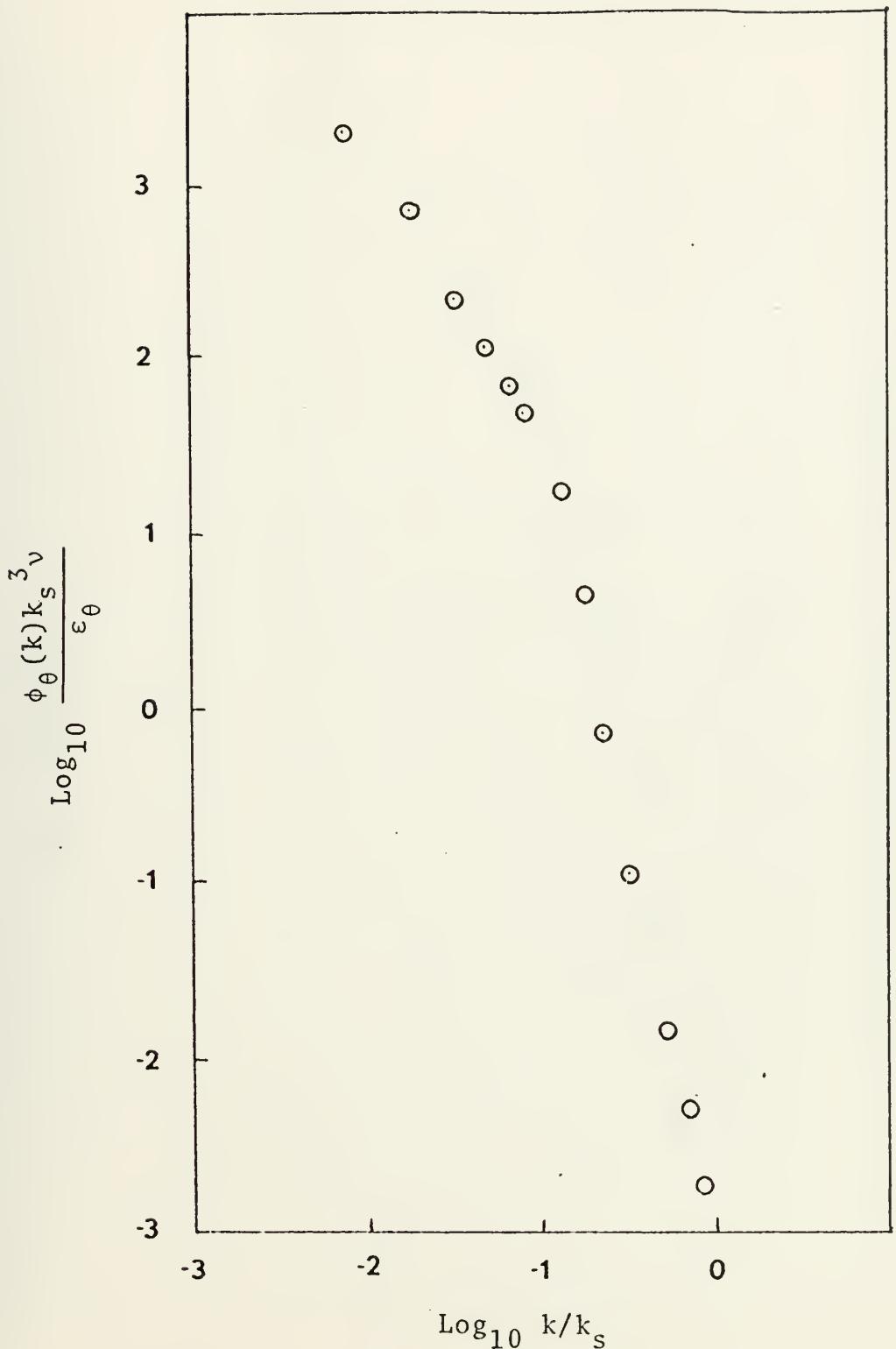
Figure 13.   Normalized NPS Temperature Spectrum
Run 6 at 7m

44

Figure 14. Normalized OSU Temperature Spectrum
Run 5 at 23m

45
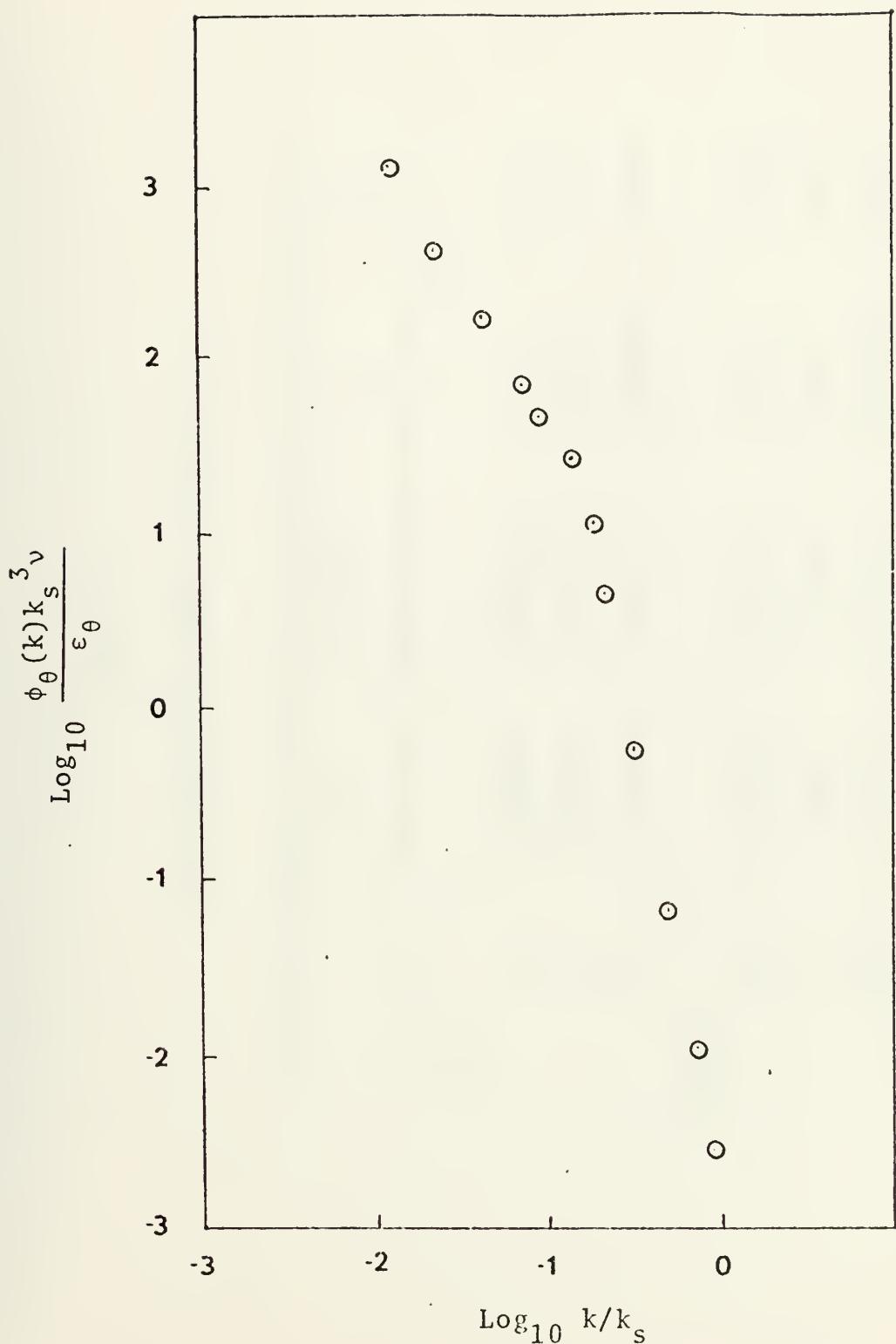
Figure 15.   Normalized OSU Temperature Spectrum
Run 6 at 23m

46

TABLE III

ONE-DIMENSIONAL SCALAR CONSTANT K_θ'

	Re	ϕ_θ(20Hz)	ϵ_θ	K_θ'
Run 5				
2m	5.25(5)	6.50(-5)	0.011	0.797
7m	2.09(6)	9.40(-5)	0.0074	0.836
23m	7.67(6)	1.80(-5)	0.00062	1.060
Run 6				
2m	5.15(5)	5.11(-5)	0.0085	0.760
7m	1.99(6)	7.14(-5)	0.0049	0.876
23m	7.16(6)	1.40(-5)	0.00048	0.948
			Average	0.880

all the spectra on a single plot (Figure 16). The break
from the -5/3 region occurs just beyond $\log k/k_s = -1$.
These spectra show the shape of the one-dimensional
temperature spectra in air beyond the -5/3 region which
was one of the primary objectives of this thesis. The
slope of the spectrum beyond the -5/3 break tended to be
-32/5 which agrees well with Heisenberg (1948) who demon-
strated that a slope of -7 should exist for very large
values of k. With the exception of the temperature
spectra at 2m, there is very little scatter in the data
at high wave numbers.

Figure 17 is a composite plot of characteristic
temperature and velocity spectra. It is noted that there
is very little difference between the two spectra but the
temperature spectrum extends to slightly higher wave
numbers than the velocity spectrum. A -32/5 slope is
observed for both temperature and velocity.

b. Temperature Dissipation Spectra

The temperature dissipation spectra were
normalized according to Eq. 9 and again plotted linearly.
Figure 18 shows a typical normalized temperature dissipa-
tion spectrum. There is very little difference between
the temperature and velocity dissipation spectra. The
normalized shapes are almost identical with the temperature
spectrum dropping off slightly faster than the velocity
spectrum.

The y-axis label reads: $\text{Log}_{10} \dfrac{\phi_\theta(k) k_s^3 \nu}{\varepsilon_\theta}$

The x-axis label reads: $\text{Log}_{10} \ k/k_s$

Legend:
△ 2m
⊙ 7m, 23m
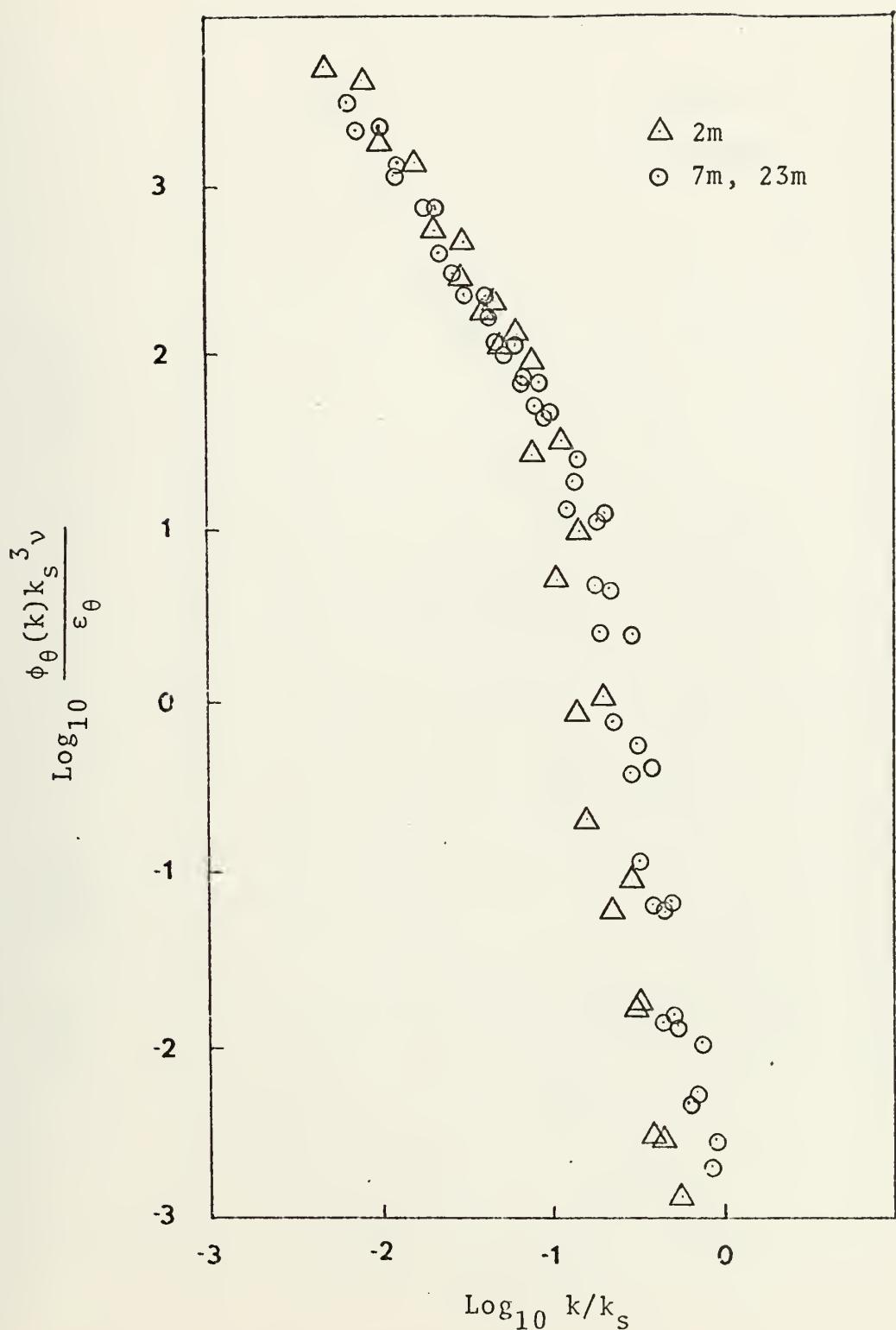
Figure 16.   Composite Normalized Temperature Spectra
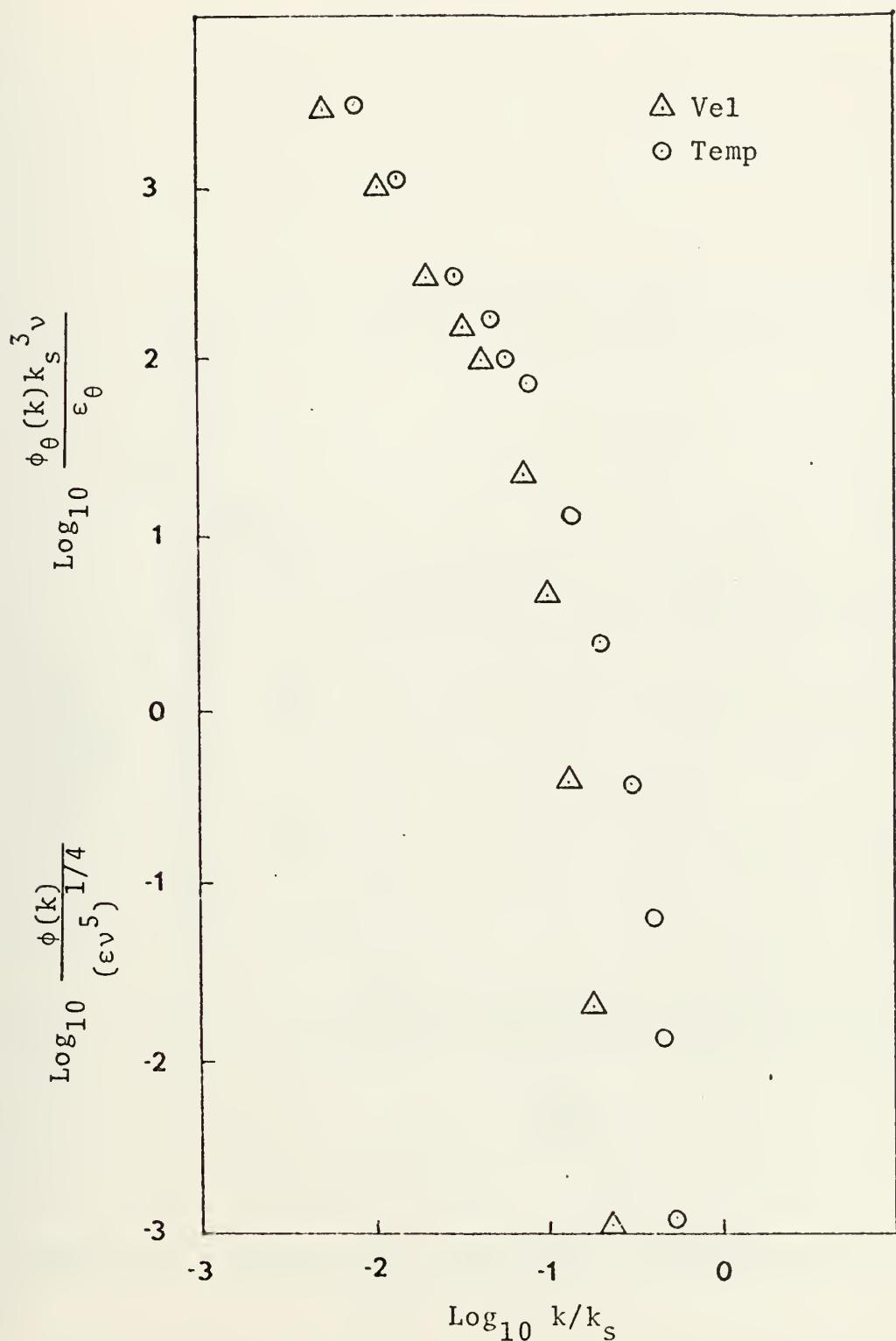
Figure 17. Comparison of Normalized Temperature and
Velocity Spectra
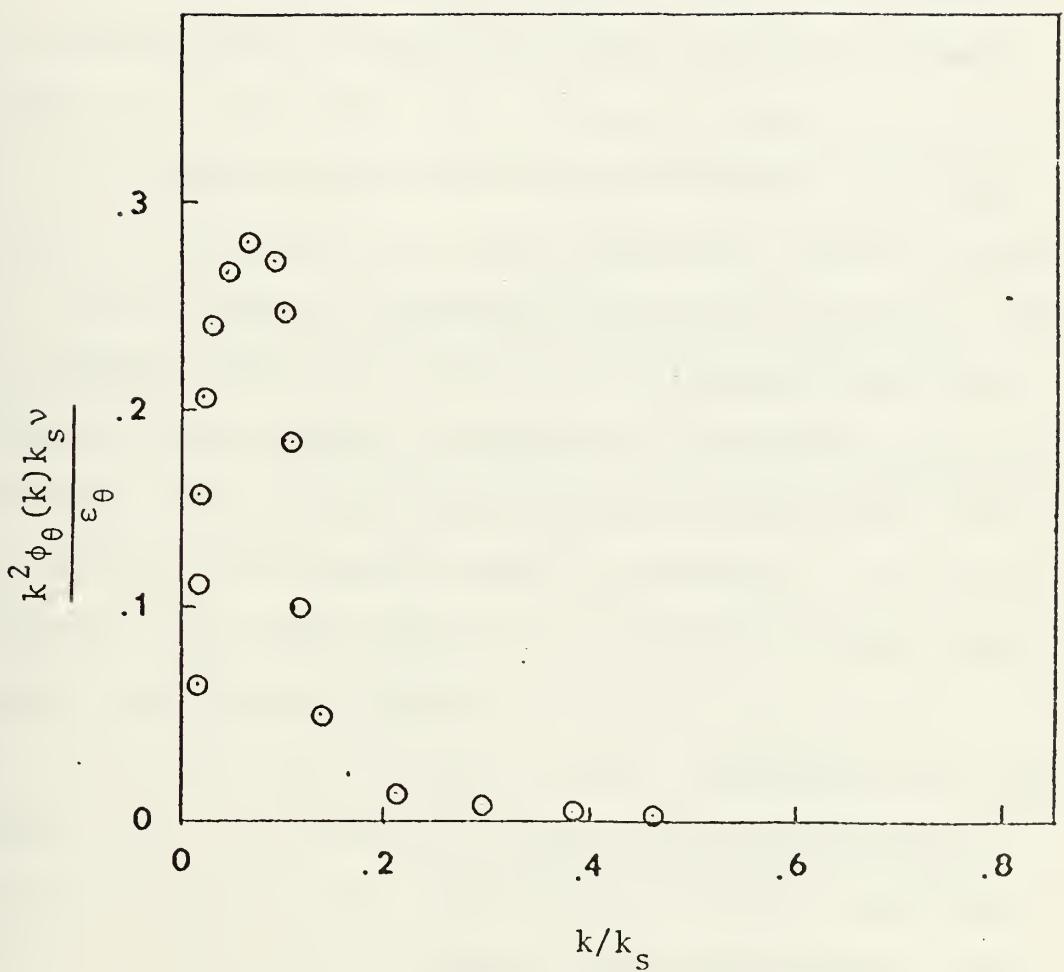
Figure 18. Normalized Temperature Dissipation Spectrum

51

VI. SUMMARY AND CONCLUSIONS

The two primary objectives of this research were to determine the shape of the high wave number one-dimensional temperature spectrum and the evaluation of the Kolmogorov scalar constant K_θ'.

As seen in the results section, this investigator has determined that the high wave number one-dimensional temperature spectrum falls off with a slope of -32/5 beyond the -5/3 break which occurs slightly beyond log k/k_s = -1. Also the determination of the Kolmogorov scalar constant, K_θ', to be 0.88 is considered to be significant not only in absolute value but also that it increases the data base of high frequency temperature fluctuation analysis. Further, the criticism that previous evaluations were based on records that were too short is removed. It was also observed (Table III) that K_θ' increased in value both with height and Reynolds Number.

As an additional result of this research, it is concluded that the spectra of temperature and velocity at high wave numbers are very similar with the temperature spectra extending to slightly higher wave numbers than the velocity spectra but that they both fall off at the same rate.

BIBLIOGRAPHY

Batchelor, G. K., "Small Scale Variations of Convected
Quantities Like Temperature in a Turbulent Fluid (Part 1)."
J. Fluid Mech. 5, p. 113-133, 1959.

Batchelor, G. K., Howells, J. D., and Townsend, A. A.,
"Small Scale Variations of Convected Quantities Like
Temperature in a Turbulent Fluid (Part 2)." J. Fluid
Mech. 5, p. 134-139, 1959.

Boston, N. E. J., An Investigation of High Wave Number
Temperature and Velocity Spectra in Air, Ph.D. Thesis,
University of British Columbia, 1970.

Corrsin, S., "On the Spectrum of Isotropic Temperature
Fluctuations in an Isotropic Turbulence." J. Appl. Phys.
22, p. 469, 1951.

Naval Postgraduate School Technical Report NPS-588Bb
72021, A High Frequency Platinum Thermometer System
for Measuring Turbulent Atmospheric Temperature
Fluctuations, by N. E. J. Boston and E. L. Sipe, 1975.

Gibson, C. H., and Schwarz, H. W., "The Universal Equilibrium
Spectra of Turbulent Velocity and Scalar Fields."
J. Fluid Mech. 16, p. 365-384, 1963.

Heisenberg, W. Z., Physik, 124, 628, 1948.

Lumley, J. L., and Panofsky, H. A., The Structure of
Atmospheric Turbulence, Wiley, 1964.

Nye, J. O., and Brodkey, R. S., "The Scalar Spectrum in
the Viscous-Convective Subrange." J. Fluid Mech. 29,
p. 151-163, 1967.

Panofsky, H. A., "The Spectrum of Temperature." Radio
Science, 4, p. 1143-1146, 1969.

Stewart, R. W., Wilson, J. R., and Burling, R. W., "Some
Statistical Properties of Small Scale Turbulence in an
Atmospheric Boundary Layer." J. Fluid Mech. 41, Part 1.
p. 141-152, 1970.

Williams, R. W., Jr., High Frequency Temperature and
Velocity Fluctuations in the Atmospheric Boundary
Layer, Ph.D. Thesis, Oregon State University, Corvallis,
1974.

Wyngaard, J. C., "The Effect of Velocity Sensitivity on
    Temperature Derivative Statistics in Isotropic
    Turbulence." J. Fluid Mech. 48, p. 763-769, 1971.

INITIAL DISTRIBUTION LIST

No. Copies

1. Defense Documentation Center   2
   Cameron Station
   Alexandria, Virginia   22314

2. Library, Code 0212   2
   Naval Postgraduate School
   Monterey, California   93940

3. Department Chairman, Code 58   3
   Department of Oceanography
   Naval Postgraduate School
   Monterey, California   93940

4. Assoc Professor N. E. J. Boston, Code 58 Bb   1
   Department of Oceanography
   Naval Postgraduate School
   Monterey, California   93940

5. Assoc Professor T. M. Houlihan, Code 59 Hm   1
   Department of Mechanical Engineering
   Naval Postgraduate School
   Monterey, California   93940

6. Commanding Officer   1
   Fleet Numerical Weather Central
   Monterey, California   93940

7. Commanding Officer   1
   Environmental Prediction Research Facility
   Monterey, California   93940

8. Department of the Navy   1
   Commander Oceanographic System, Pacific
   Box 1390
   FPO San Francisco   96610

9. Oceanographer of the Navy   1
   Hoffman II
   200 Stovall Street
   Alexandria, Virginia   22332

10. Office of Naval Research   1
    Code 480
    Arlington, Virginia   22217

11. Dr. Robert E. Stevenson   1
    Scientific Liaison Office, ONR
    Scripps Institution of Oceanography
    La Jolla, California 92037

12. Library, Code 3330   1
    Naval Oceanographic Office
    Washington, D. C. 20373

13. SIO Library   1
    University of California, San Diego
    P. O. Box 2367
    La Jolla, California 92037

14. Department of Oceanography Library   1
    University of Washington
    Seattle, Washington 98105

15. Department of Oceanography Library   1
    Oregon State University
    Corvallis, Oregon 97331

16. Dr. Carl Gibson   1
    University of California, San Diego
    Department of Ames
    P. O. Box 109
    La Jolla, California 92037

17. Dr. James J. O'Brien   1
    Program Director
    Physical Oceanography
    Ocean Science and Technology Division
    Office of Naval Research
    Arlington, Virginia 22217

18. Dr. R. M. Williams   1
    Oregon State University
    School of Oceanography
    Corvallis, Oregon 97331

19. Dr. J. Wyngaard   1
    AFCRL (LYB)
    L. G. Hanscom Field
    Bedford, Massachusetts 01730

20. LT Robert Thomas Simril, USN
    2321 Wensley Drive
    Charlotte, North Carolina 28210   2

21.   Dr. R. W. Burling   1
      Institute of Oceanography
      University of British Columbia
      Vancouver 8, British Columbia
      Canada

22.   Dr. Michel Coantic   1
      Institut de Mecanique Statistique
      de la Turbulence
      12, Avenue General Leclerc
      Marseille (3^e), France

23.   Dr. A. Gyr   1
      Institute of Hydromechanics and
      Water Resources Management
      8006 Zurich, Tannenstrasse 1
      Switzerland

24.   Dr. Søren Larson   1
      Research Establishment Risø
      DK-4000 Roskilde, Denmark